Meta-Tyrosine Induces Cytotoxic Misregulation of Metabolism in *Escherichia coli*

Nathaniel Howitz[1] Trent Su[2,3], and Beth A. Lazazzera[1,4*]
[1]Department of Microbiology, Immunology and Molecular Genetics, [2]Department of Biological Chemistry, [3]Institute for Quantitative and Computational Biology, and [4]Molecular Biology Institute, University of California, Los Angeles, California 90095, USA

Corresponding Author:
Beth A. Lazazzera
Department of Microbiology, Immunology, and Molecular Genetics
609 Charles E. Young Dr. East
1602 Molecular Science Building
University of California, Los Angeles
Los Angeles, CA 90095

(310) 794-4804 (voice)
(310) 206-5231 (fax)
BethL@microbio.ucla.edu

Running Title: *m*-tyrosine toxicity in *E. coli*
Keywords: Editing, quality control, PheRS, *m*-tyrosine, resistance mutations, *Escherichia coli,* aminoacyl-tRNA synthetase

ABSTRACT

The non-protein amino acid *meta*-Tyrosine (*m*-Tyr) is produced in cells under conditions of oxidative stress, and *m*-Tyr has been shown to be toxic to a broad range of biological systems. However, the mechanism by which *m*-Tyr damages cells is unclear. In *E. coli*, the quality control (QC) function of phenyalanyl-tRNA synthetase (PheRS) is required for resistantce to *m*-Tyr. To determine the mechanism of *m*-Tyr toxicity, we utilitized a strain of *E. coli* that expresses a QC-defective PheRS. The global responses of *E. coli* cells to *m*-Tyr were assessed by RNA-seq, and >500 genes were differentially expressed after the addition of *m*-Tyr. The most strongly up-regulated genes are involved in unfolded-protein stress response, and cells exposed to *m*-Tyr contained large, electron-dense protein aggregates, indicating that *m*-Tyr destabilized a large fraction of the proteome. Additionally, we observed that amino acid biosynthesis and transport regulons, controlled by ArgR, TrpR, and TyrR, and the stringent-response regulon, controlled by DksA/ppGpp, were differentially expressed. *m*-Tyr resistant mutants were isolated and found to have altered a promoter to increase expression of the enzymes for Phe production or to have altered transporters, which likely result in less uptake or increased efflux of *m*-Tyr. These findings indicate that when *m*-Tyr has passed the QC checkpoint by the PheRS, this toxicity of *m*-Tyr may result from interfering with amino acid metabolism, destabalizing a large number of proteins, and the formation of protein aggregates.

INTRODUCTION

Non-protein amino acids (NPAAs) are distinct from the canonical amino acids used for protein synthesis. In particular, NPAAs are toxic to humans and animals, and their presence in proteins has been correlated with neurodegenteration [1, 2]. One source of these NPAAs is biosynthetic intermediates and metabolites, for example, homocysteine, homoserine, and ornithine [3]. Another source of NPAAs is oxidatively damaged amino acids and proteins [3]. For example, reactive oxygen species (ROS) such as a hydroxyl radical can attack the *meta* position on a Tyr ring producing 3,4 dihydroxyphenylalanine (L-DOPA) or on a Phe ring producing *meta*-tyrosine (*m*-Tyr) [4]. A number of plants have been shown to produce NPAAs as a defense mechanism, highlighting the toxicity of these NPAAs when incoprorated into the proteome [5]. One mechanism by which NPAAs enter the proteome is through mischarging of tRNAs with a NPAA [6-9]. If gone unchecked, these mischarged tRNAs would provide an NPAA to the ribosome, thereby causing alteration of the protein seqence. The system-wide response of cells to NPAAs is not currently known.

The proteins that are responsible for charging tRNAs with the correct amino acids are aminoacyl-tRNA synthetases (aaRS). Some of these aaRSs (9 out of 20) have evolved QC mechanisms to deal with mischarged tRNAs [3]. One QC mechanism is pre-transfer editing, the hydrolysis of the aminoacyl adenylate prior to transfer of the amino acid to the tRNA [10]. Homocysteine, homoserine, and ornithine can be activated to form an aminoacyl adenylate that is then hydrolyzed by a pre-transfer editing reaction of MetRS, IleRS, LeuRS, and LysRS [11]. Post-transfer editing is a second QC mechanism in which a non-cognate amino acid is hydrolyzed from the tRNA either by a dedicated editing domain attached to the aaRS (*cis* editing) or a standalone protein (*trans* editing) [12-15]. The NPAAs, L-DOPA and *m*-Tyr, are

substrates for PheRS, and *m*-Tyr is also a substrate for TyrRS, but only PheRS possess an editing activity against these NPAAs [16-21].

The presence of aaRS editing domains can greatly decrease the rate of mischarging of tRNAs. For example, the phenylalanyl-tRNA synthetase (PheRS), can misactivate and mischarge $tRNA^{Phe}$ with tyrosine at a higher level than observed for the overall rate of mistranslation, but the editing domain on PheRS subsequently hydrolyzes the mischarged $tRNA^{Phe}$, bringing the level of mischarged $tRNA^{Phe}$ to that observed in translation [22, 23]. These and other data indicate that aaRS editing function is one of the last QC mechanisms before the incorrect amino acid is added to a polypeptide [24, 25].

m-Tyr incorporation into the proteome is associated with inhibition of cell growth [26]. *E. coli* are resistant to high levels of *m*-Tyr, but mutants of *E. coli* that lack the QC function of PheRS are sensitive to *m*-Tyr [18]. Rates of *m*-Tyr misincorporation into the proteome for *E. coli* increase from ~1.5% for the wild-type strain to ~2.5% for the PheRS editing-defective strain, when grown on a sub-lethal concentration of *m*-Tyr [18]. These data indicate that QC by PheRS is a critical pathway limiting the incorporation of *m*-Tyr into proteins. Whether cells have other mechanisms to prevent *m*-Tyr incorporation into proteins or to limit the toxic effects of the presence of *m*-Tyr is unknown [27]. Also unclear is why is an increase in misincorporation of only ~1% *m*-Tyr for the PheRS editing-defective strain results in such a dramatic increase in toxicity of *m*-Tyr when over 5% misincorporation of Tyr is well-tolerated [28].

Here, we address the question of how *m*-Tyr leads to cell death with a multifaceted investigation of *m*-Tyr toxicity to an *E. coli* PheRS QC-defective mutant. To reveal the global responses of cells to *m*-Tyr, we used RNA-seq to reveal changes in the transcriptome, identifying that cells exhibited induction of the unfolded-protein response, altered amino acid biosynthetic

pathways, and decreased stringent response as mediated by DksA/ppGpp. Cells exposed to *m*-Tyr formed large protein aggregates localized to the poles, indicating a large pool of unfolded protein in cells. Selection for mutants resistant to *m*-Tyr identified that the only mechanisms to resist *m*-Tyr were to alter transport of *m*-Tyr or increase production of Phe.

RESULTS

Transcriptomic Analysis of *pheT(G318W)* Cells Treated with *m*-Tyr

We used RNA-seq to reveal the global response of cells exposed to *m*-Tyr. The *pheT(G318W)* mutant strain of *E. coli* was used in this study as it exhibits increased sensitivity to *m*-Tyr and higher levels of misincorporation of *m*-Tyr in the proteome [18]. This strain was grown in minimal media, and *m*-Tyr at 0.5 mM was added when cells had reached mid-exponential growth. At this sublethal concentration of *m*-Tyr, the viable CFU/ml is reduced after 30 minutes, ranging from 10- to 40-fold, the CFU/ml then remained constant for the next 30 minutes, and after a further 60 minutes the CFU/ml had begun to increase. To understand the response of these cells to *m*-Tyr, samples for RNA extraction were taken at 0, 30, 60 and 120 minutes after *m*-Tyr treatment. When compared to cells prior to *m*-Tyr exposure (t=0), the 30-, 60-, and 120-minute time points had 577, 644 and 634 differentially expressed genes using the cut off of at least 2-fold change in expression and $p<0.005$ (Table S2). However, when compared to the previous time point, t=30 versus t=60 and t=60 versus t=120 only had 28 and 61 differentially expressed genes that made the cutoff, respectively (Table S2).

To reveal the effects of *m*-Tyr on cells, we searched the genes differentially expressed due to *m*-Tyr exposure for regulons that were enriched in the data set. Using tools at EcoCyc [29], we identified putative regulons, each associated with a particular transcriptional regulator,

that were differentially expressed. We then searched the full regulon, identified at EcoCyc, for each transcriptional regulator to determine the percent of operons in that regulon that were differentially expressed under *m*-Tyr exposure (Table 1). We considered anything with more than 50% of the operons differentially expressed as indication that the activity of the transcriptional regulator may have been affected by the presence of *m*-Tyr. From this, we identified three regulators that affect amino acid biosynthesis and transport, ArgR, TrpR, and TyrR, two regulators that are activated by unfolded proteins, Sigma-32 and CpxR, and one regulator of the stringent response, DksA-ppGpp.

Effect of *m*-Tyr on the heat sensitivity of QC-defective PheRS cells

Following the addition of *m*-Tyr, the *pheT(G318W)* cells underwent a very robust unfolded-protein response, as indicated by the induction of the Sigma-32 and CpxAR regulons (Table 2). Sixteen different operons encoding protein chaperones and proteases had very elevated levels of transcription. As *m*-Tyr induces a response typical of heat shock, these *m*-Tyr treated cells may be more resistant to heat treatment than non-*m*-Tyr-treated cells because they have already induced the proteases, chaperones, and other factors needed to resist the effects of high temperature. To test this, we grew *pheT(G318W)* and WT cells in M9 minimal media with a sub-lethal concentration of *m*-Tyr, in order to induce the unfolded-protein response. These cells were washed to remove *m*-Tyr, incubated at 60°C, and then the viable CFU/ml was periodically assessed. For cells pre-treated with *m*-Tyr, the *pheT(G318W)* cells died much more rapidly than WT upon exposed to heat (Fig. 1A). When the strains were not exposed to *m*-Tyr, both the *pheT(G318W)* and WT strains died at statistically indistinguishable rates (Fig. 1B). These data suggest that increased expression of the Sigma-32 and CpxAR regulons in the *pheT(G318W)* cells treated with *m*-Tyr was not functional in conferring resistance to heat shock.

Protein aggregate formation in the presence of *m*-Tyr

The increase in expression of Sigma-32 and CpxAR regulons indicates that the presence of *m*-Tyr in proteins may compromise the stability of the proteome. A high level of unstable, unfolded proteins in the presence of *m*-Tyr could explain the increased sensitivity to heat, which would create yet more unfolded proteins. A high level of unfolded proteins can lead to protein aggregates that are visible in cells via microscopy. To test whether protein aggregates were forming, WT and *pheT(G318W)* strains were grown in M9 minimal media and dosed with different *m*-Tyr concentrations. Sample points from each culture were taken right before the addition of *m*-Tyr (t=0), and 30, 60, 120, and 300 minutes afterwards. Cells were examined by DIC microscopy, and the *pheT(G318W)* cells exposed to *m*-Tyr developed dark spots that localized to the poles of the cells, while the WT strain showed very few polar dark spots (Fig. 1C). Additionally, the *pheT(G318W)* cells became elongated during later time points. To quantify these observed changes, 50 cells from each time point were measured and the number of large, dark spots was recorded (Fig. 1D&E). In the absence of *m*-Tyr, cells formed an average of 0.2 polar protein aggregates per cell. In contrast, after the addition of 0.1 mM *m*-Tyr, an average of 0.8 aggregates were formed per cell after 120 minutes of exposure. This level increased to 1.3 aggregates per cell at 0.5 mM *m*-Tyr. The average cell length doubled from 2.2 μm prior to *m*-Tyr exposure to 4.3 μm after 300 minutes of exposure. This cell elongation indicates that these cells exposed to *m*-Tyr are metabolically active, but are inhibited for cell division.

We hypothesized that these dark polar spots are protein aggregates formed by the cell to deal with a large number of unfolded proteins that were destabilized by the incorporation of *m*-Tyr. To test this hypothesis, we performed Transmission Electron Microscopy (TEM) on *pheT(G318W)* cells grown in M9 and exposed to 0.5 mM *m*-Tyr for 120 minutes (Fig. 1F).

Thirteen cells were analyzed by TEM, and the images revealed the same polar localization of the spots that we observed with the DIC microscopy. The spots have an electron density and disorganized shape consistent with large protein aggregates [30, 31]. The spots came in a variety of sizes; some having what appears to be satellite protein aggregates that could be in the process of being added to the larger aggregate (Fig. 1F). These results are consistent with *m*-Tyr causing large-scale proteome destabilization.

Isolation of Mutants that Resist *m*-Tyr Toxicity

In order to further understand the mechanism(s) of *m*-Tyr toxicity, we isolated mutants that are *m*-Tyr-resistant (*m*-Tyr^R) derivatives of the *pheT(G318W)* strain of *E.coli*. Cells of this strain were subjected to chemical mutagenesis with 2% ethyl methanesulfonate (EMS) and were then outgrown in either M9 minimal media or LB in the absence of *m*-Tyr. The mutagenized cells were then transferred to M9 minimal media with a sub-lethal concentration of *m*-Tyr (0.5 mM) to allow for enrichment of *m*-Tyr^R mutants. The enriched cultures were then plated onto minimal media plates with a lethal *m*-Tyr concentration (8 mM), and resistant colonies were streak purified. We performed seven independent mutagenesis assays and isolated eight unique *m*-Tyr^R strains (Table 3). Strains were designated Rmt(1-8) for "Resistant to *m*-Tyr" and the order they were isolated.

To quantify the resistance levels of the newly isolated *m*-Tyr^R mutants, they were inoculated into minimal media with a lethal *m*-Tyr concentration (2 mM) and allowed to grow at 37°C shaking for 24 hours (Fig. S1). The average final OD_{600} of the *m*-Tyr^R strains was used as a proxy for their level of resistance to *m*-Tyr. The resistance assay revealed that the strains had a variety of levels of resistance, all higher than *pheT(G318W)* negative control. Some showed resistance levels lower than the WT control, such as Rmt1, Rmt2, and Rmt4. Contrastingly,

Rmt5 and Rmt7 showed greater than WT levels of growth. Most of the *m*-Tyr^R strains had a higher variance in their final OD_{600} than the WT control indicating that their mechanisms of resistance could be more stochastic than quality control by PheRS that is responsible for resisting *m*-Tyr.

We performed whole-genome sequencing on the eight strains and the *pheT(G318W)* parental strain, and searched for SNPs that could explain the strains' resistance to *m*-Tyr. Sample genomic DNA was sequenced using the Illumina® NextSeq™. SNPs were identified with a minimum requirement of 5x coverage of a given base and 80% agreement on the mutation. In total, there were 156 non-silent and intergenic SNPs identified across the eight unique strains (Table S3). Notably, there were no WT revertants among them. Candidate *m*-Tyr^R mutations were identified by searching for genes and loci that were mutated in multiple strains. Four of the eight mutants had a mutation in *aroP*, and three of the eight had a mutation in *rthC*, suggesting that these were possible mutations conferring *m*-Tyr^R (Table 3). The eighth strain, which did not have an *aroP* or *rhtC* mutation, had only five SNPs, and the mutation in *tyrA* was most probable SNP to be responsible for the *m*-Tyr^R as TyrA is required for Tyr and Phe biosynthesis (Table 3).

Loss of Function Mutations in *aroP* Imparts Resistance to *m*-Tyr

The aromatic amino acid transporter gene *aroP* was mutated in 4/8 of the *m*-Tyr^R strains. These mutations all appeared to be loss-of-function mutations, two of which are nonsense mutations truncating the protein to either 42 or 100 residues long (Table 3). To test if loss of AroP conferred *m*-Tyr resistance, we introduced an Δ*aroP* allele into the *pheT(G318W)* strain and tested for resistance to *m*-Tyr. This strain showed elevated *m*-Tyr resistance compared to the isogenic *pheT(G318W)* strain (Fig. 2A). To further assess the contribution of the *aroP* mutations to the resistance of the Rmt strains, we replaced the mutated *aroP* alleles with an *aroP*$^+$allele in

the Rmt strains and tested the *m*-Tyr resistance of the resulting strains (Fig. 2A). Three of the four Rmt *aroP*$^{+}$ strains (Rmt1, Rmt3, and Rmt6) showed severely reduced *m*-Tyr resistance as compared to their Rmt parent strain. The 4th strain, Rmt2 *aroP*$^{+}$, showed extremely variable levels of *m*-Tyr resistance. These data indicate that loss-of-function mutations in *aroP* confer *m*-Tyr resistance, presumably by reducing the rate of import of *m*-Tyr.

rhtC Promoter Mutation Imparts Resistance to *m*-Tyr

RhtC has been reported to be a threonine efflux pump [32, 33]. In our *m*-Tyr^{R} screen, a mutation (C-43T) that is 43-bp upstream of the gene *rhtC* was isolated three times independently in Rmt4, Rmt5, and Rmt7. The (C-43T) mutations is located 1-bp downstream of the -35 promoter sequence and 10-bp upstream of the -10 promoter sequence. We tested the requirement of *rhtC* for *m*-Tyr resistance by deleting the (C-43T) mutation and the *rhtC* open-reading frame (*rhtC*Δ-59-621) in the Rmt4, 5 and 7 strains. In all three strain backgrounds, introduction of this deletion eliminated *m*-Tyr resistance (Fig. 2B). We also inserted the *rhtC* (C-43T) mutation into the orginal *pheT(G318W)* strain, which provided the strain with a level of *m*-Tyr resistance similar to the the Rmt4, 5 and 7 mutants (Fig. 2B). To determine whether the *rhtC* (C-43T) mutation was sufficient to cause resistance or whether the *rhtC* open reading frame was also necessary, we introduced a deletion of *rhtC* that left the (C-43T) mutation in place (*rhtC*Δ0-621) into the Rmt 4, 5, and 7 mutants. These mutants were found to be as sensitive to *m*-Tyr as the *pheT(G318W)* strain (Fig. 2B). These data indicate that the *rhtC*(C-43T) mutation is a gain-of-function mutation, as loss of *rhtC* did not phenocopy the Δ*rhtC* mutation. As RhtC is an efflux pump for threonine, the simplest model for how the *rhtC*(C-43T) mutation increases *m*-Tyr resistance is that the C-43T mutation increases expression of *rhtC* and causes efflux of *m*-Tyr.

Mutation in *tyrA* Imparts Resistance to *m*-Tyr

One *m*-Tyr^R strain, Rmt8, had 5 mutations, and of these mutations, the *tyrA(G106S)* mutation was the most likely to be involved in m-Tyr resistance. The other mutations affected genes involved in carbon or nucleotide metabolism or a gene of unknown function (Table S3). In contrast, *tyrA* encodes a bifunctional chorismate mutase-prephenate dehydrogenase, that is required for tyrosine and phenylalanine biosynthesis [34]. To determine whether the *tyrA(G106S)* mutation was required for *m*-Tyr resistance in Rmt8, the *tyrA(G106S)* allele was replaced with the wild-type *tyrA* allele (*tyrA*$^+$). The Rmt8 (*tyrA*$^+$) strain was tested for *m*-Tyr resistance and found to be as sensitive to *m*-Tyr as the parental *pheT(G318W)* strain (Fig. 2C). To determine whether the *tyrA(G106S)* mutation was sufficient to cause *m*-Tyr resistance, the WT allele of *tyrA* was replaced with the *tyr(G106S)* allele in the *pheT(G318W)* strain. The resulting *pheT(G318W), tyrA(G106S)* strain showed the same level of *m*-Tyr resistant as the Rmt8 mutant strain (Fig. 2C). The *tyrA(G106S)* mutation is not a loss-of-function mutation, as strains with the *tyrA(G106S)* allele grew in minimal medium lacking Tyr, and *tyrA* is required for growth in the absence of exogenously added Tyr. Thus, the *tyrA(G106S)* mutation contributes to *m*-Tyr resistance by altering the function of TyrA, presumably to increase the pools of phenylalanine in the cell.

DISCUSSION

The non-protein amino acid *m*-Tyr, which is produced under oxidative stress conditions, is toxic to cells. The mechanism of this toxicity and the means by which cells resist this toxicity is not fully known. Here we reveal the stress responses that are induced in response to *m*-Tyr toxicity are an unfolded-protein response, general stress response, and dis-regulation of amino acid biosynthetic pathways. Resistance to *m*-Tyr was found to evolve through mutations in genes for transporters that likely modify uptake or efflux of *m*-Tyr, and in a gene involved in tyrosine and phenyalanine biosynthesis. These data indicate that the QC of PheRS is the main mechanism by which *E. coli* cells resist *m*-Tyr. We futher find that if *m*-Tyr bypasses the QC of PheRS, it will enter proteins that will become unfolded and become aggregated in inclusion bodies at cell poles, which we propose to be the secondary mechanism by which cells resist *m*-Tyr.

m-Tyr Inhibition of the Stringent Response

Previous work showed that in response to starvation for phenyalanine, cells lacking QC by PheRS continued to aminoacylate $tRNA^{Phe}$, which caused these cells to have reduced levels of ppGpp, the stringent response alarmone [35]. Low levels of ppGp are a response to uncharged tRNAs at the ribosome. It was further shown that a gene activated by ppGpp and a gene repressed by ppGpp had altered regulation due to the lack of QC by PheRS which was exacerbated by the presence of *m*-Tyr [35]. Here we observed, in the absence of amino acid starvation, that *m*-Tyr addition led to broad induction of genes repressed by stringent response through DksA and ppGpp (Table S4). Of 33 operons controlled by DksA/ppGpp, 19 are differentially expressed, with repressed genes being induced and activated genes being downregulated. Of the 14 DksA/ppGpp operons that did not show this pattern of gene

expression, six of these are the ribosomal RNA (rRNA) operons, and rRNA was specifically removed from the cellular RNA used for this RNA-seq analysis. Overall, these data strongly support the presence of *m*-Tyr in reducing the basal levels of the stringent response that is present even in cells that are not experiencing amino acid starvation. This data would indicate the PheRS QC-defective cells are producing ribosomal proteins, and presumably ribosomes, at a higher rate than cells that are not exposed to *m*-Tyr. The consequence of this increased protein synthesis capactity would be a faster rate of *m*-Tyr being incorporated into proteins, more unfolded proteins being produced, which likely contributes to the toxicity of *m*-Tyr.

Why in the absence of amino acid starvation does *m*-Tyr lead to reduction in the stringent response? There is very likely a small pool of uncharged tRNAs in the cell even during active growth. The presence of *m*-Tyr, which can be aminoacylated to both $tRNA^{Phe}$ and $tRNA^{Tyr}$, should reduce the size of the pool of uncharged tRNAs, leading to fewer stalled ribosomes, and less RelA produced ppGpp. This could lead to derepression of of DksA/ppGpp-regulated operons that encode ribosomal proteins and rRNAs.

m-Tyr Alteration of Amino Acid Biosynthesis

The addition of *m*-Tyr to the *pheT(G318W)* mutant cells altered regulation of genes controlled by the transcription factors ArgR, TrpR, and TyrR. ArgR inhibits the expression of enzymes involved in the production of arginine [36], and these genes were significantly up-regulated in the presence of *m*-Tyr, indicating that ArgR was inactivated. ArgR was found to be particularly sensititve to inactivation by exposure to peroxynitrite. This sensitivity occurred through nitration of tyrosine residues [37]. Possibly, the misacylation of $tRNA^{Phe}$ with *m*-Tyr and incorporation of *m*-Tyr in ArgR in place of Phe could result in similar inactivation of ArgR.

Alternatively, the misacylation of $tRNA^{Tyr}$ with *m*-Tyr could be the cause for inactivation of ArgR, as $tRNA^{Tyr}$ has been shown to be aminoacylated with *m*-Tyr by TyrRS [18].

TrpR and TyrR are transcription factors that regulate tryptophan and aromatic amino acid biosynthesis and transport, respectively [38, 39]. The genes repressed by these transcription factors are downregulated in the presence of *m*-Tyr, indicating that both the TrpR and TyrR transcription factors are activated by the presence of *m*-Tyr. TyrR is activated by binding either Tyr or Phe , and it is very likely that *m*-Tyr binds TyrR as well. The activation of TyrR leads to the repression of *tyrA* and *tyrB*, enzymes that participte in both Tyr and Phe synthesis, and *aroF* and *aroG,* enzymes required for chorismate synthesis, the precursor of aromatic amino acid biosynthesis. The mechanism by which TrpR is activated by *m*-Tyr is likely indirect, possibly by increasing the production of Trp versus Tyr and Phe. TrpR represseses the *trpABCDE* genes required for Trp synthesis. The genes for other enzymes involved in aromatic amio acid biosynthesis that are repressed by *m*-Tyr are *aroA, aroD, aroE,* and *aroH,* required for chorismate synthesis, and *pheA*, required for Phe synthesis. These data indicate that the presence of *m*-Tyr, most likely throrugh its ability to act as a mimic for Tyr and/or Phe, shuts down aromatic amino acid biosythesis. A similar decrease in the pools of phenylalanine have been observed in plants after treatment with *m*-Tyr [40]. The subsequent reduction in the pools of Phe and Tyr will then increase the frequency with which *m*-Tyr will be utilized by PheRS and TyrRS in aminoacylating their cognate tRNAs, and thus the frequency of *m*-Tyr in proteins.

Induction of an unfolded protein response by *m*-Tyr

Global transcriptome analysis showed that exposure of cells lacking QC by PheRS to a sublethal concentration of *m*-Tyr resulted in induction of genes controlled by Sigma-32, the heat-shock sigma factor, and CpxAR, the periplasmic-stress two-component regulatory system [41,

42]. A simple model to explain the induction of Sigma-32 and CpxAR activity is that *m*-Tyr has led to protein unfolding in both the cytoplasm and the periplasm. Consistent with this, we saw inclusion bodies at cell poles after exposure to *m*-Tyr. Two small heat-shock proteins (sHSPs), IbpA and IbpB, associate with and disaggregate inclusion bodies/protein aggregates [43-45]. The mRNAs for these sHSPs were induced by more than 3,000-fold and were the most highly upregulated genes after *m*-Tyr treatment. Cells treated with *m*-Tyr were also longer than untreated cells, suggesting that cell-division is blocked in cells responding to *m*-Tyr. Intreguingly, IbpA and IbpB were found to be required for inhibition of cell division when their expression was induced by overexpression of the NlpI lipoprotein [46]. The unfolded protein response caused by *m*-Tyr was not catastrophic for cells as they eventually resumed normal growth and the frequency of inclusion bodies decreased. However, other stresses that induced unfolded proteins were found to have an additive effect with *m*-Tyr on the toxicity to cells, as *m*-Tyr-exposed cells died more rapidly after exposure to a lethal temperature.

After addition of *m*-Tyr, cells halted growth for one hour and then growth resumed. This raises the question of how the cells are able to recover from *m*-Tyr toxicity. We observed that the maximal number of cells with protein aggregates occurred 120 minutes after *m*-Tyr exposure, and then the level declined. Sequestration of protein aggregates to the poles of cells and then dilution of the aggregates in the population by cell division has been proposed as a protective mechanism [47-50]. Such sequestration of *m*-Tyr in protein aggregates could effectively eliminate *m*-Tyr from the cellular environment.

Mechanisms of resistance to *m*-Tyr toxicity

Previous work has demonstrated that one major way that cells resist *m*-Tyr is through the QC function of PheRS, as loss for PheRS QC results in increased sensitivity to *m*-Tyr [18]. One

outstanding question was whether cells have additional mechanisms to resist *m*-Tyr. *Caenorhabditis* elegans was recently shown to up-regulate a tyrosine aminotransferase to degrade *m*-Tyr [51]. To identify mechanisms that *E. coli* cells use to resist *m*-Tyr, we hypothesized that resistance mechanisms could be made more active through mutations. Therefore, if we could find mutant that resulted in increased *m*-Tyr resistance, the mutations harbored in the mutant strains would reveal the latent *m*-Tyr resistance mechanisms in *E. coli*. All three mutations identified in this study appear to resist *m*-Tyr by increasing the intracellular ratio of Phe to *m*-Tyr. One mutation identified was a loss-of-function mutation in *aroP*, an aromatic amino acid importer, which likely decreases transport of *m*-Tyr into the cells. Another mutation is a gain-of-function mutation in the promoter region of *rhtC*, an efflux pump for threonine, which we propose also exports *m*-Tyr from the cell. The third mutations was also a gain-of-function mutation in *tyrA*, which is an enzyme with both chorismate mutase and prephenate dehydrogenase activities that are required for Tyr and Phe biosynthesis [52]. The *m*-Tyr^R mutation in *tyrA* is predicted to decrease prephenate dehydrogenase activity, which would increase the levels of prephenate. As prephenate feeds into the Phe biosynthetic pathway, the intracellular Phe concentration may be increased, which could compete with *m*-Tyr for PheRS. Similarly, exogenous supplementation with Phe could partially rescue root growth of plants grown in soil with *m*-Tyr [53]. Also, an *A. thaliana* mutant was reported to resist *m*-Tyr by increasing Phe production [54]. While these types of mutations represent mechansims that cells have to resist *m*-Tyr, these mutations would all come with the consequence of altering the levels of other aromatic amino acids. Thus, our data argues for the central importance of the the QC function of PheRS in resisting the toxicity of *m*-Tyr.

In summary, *m*-Tyr is highly toxic to the proteome of cells and induces a strong unfolded-protein response. These *m*-Tyr-containing, unfolded proteins form inclusion bodies, which we propose is a mechanism of cells to sequester this toxic amino acid. The significant problems caused by *m*-Tyr to the proteome are resisted by the QC function of the PheRS. Mutations that alter the ratio of Phe and Tyr to *m*-Tyr can resist the toxicity of *m*-Tyr , but may have undesireable consequences on aromatic acids levels in the absences of *m*-Tyr. The toxicity of *m*-Tyr extends beyond causing unfolded proteins to alteration of the stringent response and aromatic acid biosynthesis and transport. This research thus highlights the potential problems that can result from non-protein amino acids mimicing proteogenic amino acids as regulators of enzymes and transcription factors.

MATERIALS AND METHODS

Media and Growth Conditions

For transformations into cells expressiong λ-red fuctions, LB media was used with half the normal concentration of NaCl (5 g/l). For transformations removing the *cat-sacB* cassette, LB media with 5% sucrose and lacking NaCl was used. Where indicated, cells were grown in M9 minimal media containing 0.2% glucose and M63 minimal media plates with 8 mM *m*-Tyr [55]. Ampicillin (Amp) was used at a concentration of 100 μg/ml, and chloramphenicol was used at a concentration of (10 μg/ml). Liquid media cultures were inoculated to an OD_{600} of 0.01 and either placed in a roller drum (large test tubes) or shaking (250 or 500 ml Erlenmeyer flask) at 37°C, unless otherwise noted. Overnight growth lasted 16-18 hours at 37°C or 24 hours at 28°C, unless otherwise noted.

m-Tyr^R Mutant Isolation

Chemical mutagenesis was performed using ethyl methanesulfonate (EMS) on the *E. coli pheT(G318W)* strain (BAL4073) [18]. Cells were grown overnight in LB media, and then cells from 2 ml of the culture were harvested by centrifugation and resuspended in the same volume of M9 minimal media. EMS was added to a concentration of 2%, and cells were incubated for 40 minutes with shaking at 37°C. The EMS was then removed by washing the cells five times with M9 media. The washed cells were resuspended in 2 ml of either LB or M9 media, diluted 1:10 into 20 ml of either LB or M9 media as appropriate, and the incubated with shaking at 37°C for 16 hours. In order to enrich for resistant mutants, the overnight cultures were used to inoculate 5 ml of M9 media containing 0.5 mM *m*-Tyr (sub-lethal concentration) and incubated for 16 hours with shaking at 37°C. To select for resistant mutants, the enrichment cultures were plated on plates containing M63 minimal media and 8 mM *m*-Tyr and incubated at 37°C for 16 hours.

Colonies were streak purified on plates containing 8 mM *m*-Tyr. This chemical mutagenesis protocol was repeated seven times. Resistant mutant strains were name Rmt1, Rmt 2, Rmt3, etc., for resistant to *m*-Tyr mutant 1, 2, 3, etc. With the exception of resistant strains Rmt1 and Rmt2, all identified resistant strains were isolated from independent mutagenesis reactions to ensure each strain arose independently.

Assay for *m*-Tyr Resistance

In order to assess the level of resistance to *m*-Tyr, three cultures from individual colonies of a strain were grown in LB overnight. Cells were then washed, resuspended in 0.9% NaCl, and used to inoculate three 1 ml M9 + 2 mM *m*-Tyr cultures to an OD_{600} of 0.01 in small test tubes. The cultures were then allowed to grow with shaking at 37°C for 24 hours. The growth of the cultures as measured by their final OD_{600} was used as a proxy for a strain's level of *m*-Tyr resistance.

Genome Sequencing of *m*-Tyr^R Strains

Genomic DNA samples were prepared from LB overnight cultures started from single colonies of the eight *m*-Tyr^R strains (Rmt1 to Rmt8) and the *pheT(G318W)* strain from which the Rmt mutants were derived. The MasterPure™ DNA Purification kit from Illumina® was used to isolated genomic DNA, according to the manufacturer's protocol. Genomic DNA was digested enzymatically and labeled via barcode ligation onto the ends of DNA fragments using the Illumina® TruSeq® DNA PCR-Free Library Preparation Kit, according to manufacturer's instructions. The samples were then sequenced using the Illumina® NextSeq™ with 75 bp long, pair-end reads at the USC Epigenome Center. The sequences were sorted to their correct strain automatically using a custom python script (gift of F. Seidl and S.E. Finkel at USC). The sequences were aligned to the *E. coli* MG1655 reference genome (NC_000913) using Burrow-

Wheeler Aligner and SAMtools [56, 57]. SNPs were identified with a minimum requirement of 5x coverage of a given base and 80% agreement on the mutation.

Strain Construction

In order to test candidate *m*-Tyr^R mutations identified by genome sequencing, mutated genes in the Rmt mutants were replaced with the wild-type allele. In addition, the mutant allele of genes from the Rmt mutants were introduced into the *pheT(G318W)* mutant strain. These allele replacements were performed in a two-step process in which the candidate genes were deleted and replaced with the *cat-sacB* cassette. In the subsequent step, the *cat-sacB* allele was removed via counter-selection and replacement with either the wild-type allele or the mutant allele of the candidate gene, as appropriate. All recombinations were induced by λ-red recombineering by introduction of pSIM6 into Rmt mutants and the *pheT(G318W)* strain [58].

Linear DNA products were constructed by PCR that contained the *cat-sacB* cassette flanked by 30-40 bp of homology to the target loci (see Table S1 for a list of primers). Electrocompetent cells were prepared of either the Rmt mutants or the *pheT(G318W)* mutant strain containing pSIM6 and transformed with at least 100 ng of PCR product, as previously described [59]. Transformed cells were allowed to recover for 1 hour in 1 ml of LB with shaking at 28°C, plated on LB containing chloramphenicol, and then incubated at 28°C for 24 hours. Transformants contained the *aroP::cat-sacB*, *tyrA::cat-sacB*, or *rhtC::cat-sacB* alleles and were then steak purified and checked by PCR.

In order to remove the *cat-sacB* cassette and replace it with the desired target gene allele, a double-strand DNA product of the allele was produced by colony PCR using primers homologous to at least 40 bp outside of the *cat-sacB* insertion site in target gene (Table S1). The strains containing the *cat-sacB* insertion with the pSIM6 plasmid were transformed as described

above. Transformed cells were recovered for 5 hours in 10 ml of LB lacking NaCl with shaking at 28°C. Transformants were then plated on LB + 5% sucrose plates and incubated at 28°C for 24 hours, streak purified, and tested by PCR. The pSIM6 plasmid was cured from the transformed strains by successive streak purification on LB plates grown at 37°C. Colonies were tested for the loss of the plasmid by patching on LB and LB with ampicillin plates.

Assay for Thermosensitivity

In order to test if *m*-Tyr increased the sensitivity of cells to heat, strains were assayed for their rate of cell death at a non-permissive temperature. Overnight cultures of BAL4074 (WT) and BAL4073 (*pheT(G318W)*) [18] were washed and resuspended with 0.9% NaCl and used to inoculate 5 ml M9 + 0.5 mM *m*-Tyr cultures to an OD_{600} of 0.01. These cultures were grown for 16 hours with shaking at 37°C, after which cells from the cultures were washed and resuspended in 0.9% NaCl to an OD_{600} of 1.0. Five 100 µl aliquots of serial dilutions 10^{0}-10^{-6} in 0.9% NaCl were aliquoted into PCR tubes. The tubes were incubated in a thermocycler, which ramped from room temperature to hold at 60°C. When the heating block reached 60°C (t=0), the first time-point tubes were removed and placed on ice. Tubes were removed and placed on ice every minute up to 4 minutes. Each tube was plated on LB plates, including a tube that did not go in the thermocycler, and the CFU/ml at each time point was assessed.

RNA-seq of *E. coli pheT(G318W)* Exposed to *m*-Tyr

A 5 ml LB culture was inoculated from a single colony of BAL4073 (*pheT(G318W)*) strain and grown until it reached mid-log phase (OD_{600} 0.4-0.6). A 1 ml sample of the cells were then washed in 0.9% NaCl and used to inoculate a 100 ml, M9 minimal media culture in a 500 ml flask to an OD_{600} of 0.001. The M9 culture was allowed to grow with shaking at 37°C until it reached an OD_{600} of 0.5. A sample of cells was taken at this time (t=0) for RNA purification and

CFU/ml determination. A *m*-Tyr solution was then added to the culture to 0.5 mM. The culture was then allowed to continue growing at 37°C with shaking. Additional sampling for RNA purification and CFU/ml measurements was done at 30, 60, and 120 minutes after *m*-Tyr addition. This protocol was repeated for a total of three biological replicates.

RNA purification was performed using the Qiagen® RNeasy® Mini Kit. One-ml of culture was removed for each time point and mixed with 2 ml of RNAprotect® Bacterial Reagent. RNA was then purified according to the Qiagen® protocols for "Enzymatic Lysis of Bacteria" and "Purification of Total RNA from Bacterial Lysate Using the RNeasy® Mini Kit". RNA quality was assessed using the Agilent 2100 Bioanalyzer (Santa Clara, CA, USA). Any residual genomic DNA in the RNA samples was digested using the Ambion® DNA-*free*® kit (Waltham, MA, USA). Ribosomal RNA was removed from the RNA samples using the Thermo Fisher Scientific RiboMinus™ Transcriptome Isolation Kit for bacteria. The resulting rRNA-depleted samples were then concentrated using the Qiagen® RNeasy® columns using the "RNA Clean Up" protocol. cDNA libraries were then created using New England Biolabs' (Ipswich, MA, USA) NEBNext® Ultra™ Directional RNA Library Prep Kit for Illumina® and the Primer Set 1 of NEBNext® Multiplex Oligos for Illumina (Ipswich, MA, USA). The quality of the cDNA libraries was assessed using the Agilent 2100 Bioanalyzer. Sequencing of the 12 cDNA libraries was performed using the Illumina MiSeq Personal Sequencer System with paired end 150 bp reads. RNA-seq data reported here are available at GEO, under the series GSE140211 (https://www.ncbi.nlm.nih.gov/geo/query/acc.cgi?acc=GSE140211).

Sequence results were aligned to *E. coli* str. K-12 substr. MG1655 ASM584v2.32 genome sequence using TopHat [60]. Transcript read counts were determined using HTSeq version 0.6.1p1 [61]. Normalization of read counts and differential gene expression analysis

were performed using R package DESeq2 [62]. Results were analyzed by pairwise comparison of time-points t=30, 60, and 120 to t=0. Also, the comparisons of t=30 vs. t=60 and t=60 vs. t=120 were used to assess the statistical significance of changes in gene expression over the time course.

DIC Microscopy

In assessing whether *m*-Tyr induced a visible phenotype in cells, we observed cells using Differential Interference Contrast microscopy as a function of their time of exposure to *m*-Tyr. A 5-ml LB culture was inoculated with a single colony of either the BAL4074 (WT) or BAL4073 (*pheT(G318W)*) and grown until it reached mid-log phase (OD_{600} 0.4-0.6). Cells were then washed in 0.9% NaCl and inoculated a 100-ml M9 minimal media culture in a 500 ml flask to an OD_{600} of 0.001. The M9 culture was allowed to grow with shaking at 37°C until it reached an OD_{600} of 0.5. A sample of cells was taken at this time (t=0) for imaging. A *m*-Tyr solution was then added to a final concentration of 0.1 or 0.5 mM. The control cultures received the same volume of sterile ddH_2O. Additional samples for imaging were taken 30, 60, 120, and 300 minutes after the addition of *m*-Tyr. Samples were concentrated 10-fold in M9 media, and 3 μl of the concentrated sample was then pipetted onto a 1% agarose pad, which contained the same concentration of salts as the M9 growth media, and covered with a coverslip. The cells were imaged with a Zeiss (Jena, Germany) Axioskop 2 DIC microscope, and the images were saved in ZVI format. For each image, the cell length and the number of visible dark spots of 50 cells with clearly distinguishable borders were quantified using ImageJ with the Fiji plugin [63, 64].

Transmission Electron Microscopy

A 100-ml M9 + 0.5 mM *m*-Tyr culture of the BAL4073 (*pheT(G318W)*) strain was prepared as described above in the DIC Microscopy method. Two hours after the *m*-Tyr was

added to the culture, 2 ml of culture was spun down and resuspended in 200 µl Phosphate Buffered Saline (PBS). Glutaraldehyde was added to the cell suspension to a 2% final concentration for chemical fixation. Droseran, LLC (Pasadena, CA, USA) prepared and imaged the fixed samples. 50 µl aliquots were spun down at 3,000 RPM for 2 minutes and washed twice in ddH_2O. Osmium tetroxide was added to the sample to a 1% concentration and allowed to incubate for 30 minutes. The pellet was then washed twice with ddH_2O and spun down. Uranyl acetate was then added to the sample to a final concentration of 0.5% and incubated for 30 minutes. The sample was then washed twice with ddH_2O. The sample was then incubated in increasing concentrations of ethanol (25%, 50%, 75%, 90%, and twice with 100%) for 10 minutes each. The sample was then incubated in 25% Epon uncatalyzed overnight. The next day the sample was incubated in 75% Epon for 3 hours, then in 100% Epon. The sample was then polymerized at 60°C for 24 hours. The sample was sectioned, and then imaged using an FEI Morgagni 268 at 80kV acceleration voltage.

ACCESSION NUMBER

GenBank accession number for RNA-Seq data: **GSE140211**.

ACKNOWLEGEMNTS

We thank Steve Finkel (University of Southern California) for assistance with DNA Sequencing, and Mike Ibba (Ohio State University) for critical reading of the manuscript. This work was support by an grant from NSF (MCB-1716475).

TABLE 1. Regulons differentially expressed in presence of *m*-Tyr.

Response	Transcriptional regulator	No. of operons in the regulon	% of the regulon differentially expressed	Direction of the change in gene expression		Regulator is activated or inactivated
				Repressed genes	Activated genes	
Unfolded protein	CpxR	36	61%	decreased	increased	activated
	Sigma-32	79	56%	N/A	increased	activated
Stringent	DksA-ppGpp	33	58%	increased	N/A	inactivated
Amino acid starvation	ArgR	16	75%	increased	N/A	inactivated
	TrpR	5	80%	decreased	N/A	activated
	TyrR	8	50%	decreased	increased	activated

Table 2. Sigma-32- and CpxAR-Regulated Genes Differentially Expressed by *m*-Tyr

Operon	Function	Fold Change[a]		
		t=30	t=60	t=120
Activated by Sigma-32				
ackA	acetate kinase	4.2	6.2	5.4
bssS	regulator of biofilms	22	50	65
clpB	Protein chaperone	52	110	94
clpP-clpX	ClpXP protease complex	2.5	4.9	5.1
dnaK-dnaJ	DnaK-DnaJ-GrpE chaperone system	120	170	140
fxsA	inner membrane protein	22	29	15
groS-groL	GroEL-GroES chaperonin complex	69	95	57
grpE	DnaK-DnaJ-GrpE chaperone system	22	38	35
hslV-hslU	HslVU protease	80	110	84
hspQ	hemimethylated DNA-binding protein	26	47	56
htpG	chaperone, HSP90 family	16	30	27
htpX	Heat shock protein	60	78	92
ibpA-ibpB	molecular chaperones	3400	3200	1400
lapAB	lipopolysaccharide assembly	7.5	9.7	13
lon	protease	7.3	12	9.0
miaA-hfq-hflXKC	tRNA(i6A37) synthase, RNA-binding protein, ribosome-dissociating factor, regulator of FtsH protease	16	17	12
mlc-ynfK	Regulator of PTS and PEP systems, predicted dethiobiotin synthetase	6.7	12	12
mutM	base excision repair	11	33	61
narP	nitrate/nitrite response regulator	5.2	11	19
raiA	stationary phase translation inhibitor	30	13	9.2
rlmE-ftsH	methylation of 23S rRNA, metalloprotease	19	25	18
rpmE	50S ribosomal subunit	32	42	27
rpoD	Sigma 70	3.3	7.5	11
sdaA	L-serine degradation	150	280	280
ybbN	chaperone and protein oxidoreductase	14	30	42
ybeD	conserved protein	44	67	46
ybeZYX-int	putative ATPase, maturation of 16S rRNA, transport protein, and lipoprotein maturation	9.0	10	7.7
yceI	Predicted protein	10	6.9	7.7
ycjX	Conserved protein	26	39	39
yrfG-hslRO	purine nucleotidase, heat shock protein Hsp15, Hsp33 chaperone	7.3	16	20
Activated by CpxAR				
cpxP	adaptor for DegP protease & negative regulator of	120	110	110

	CpxAR			
degP	periplasmic serine protease	85	82	50
dgcZ	diguanylate cyclase	140	120	56
ftnB	predicted ferritin-like protein	27	8.8	5.9
ldtC	removal of the D-alanine residue of peptidoglycan	59	57	39
ppiA	peptidyl-prolyl cis-trans-isomerase	9.2	7.6	3.3
rdoA-dsbA	serine/threonine protein kinase, protein disulfide oxidoreductase	22	17	17
rpoH	Sigma-32	11	13	14
spy	periplasmic chaperone	77	69	95
tomb-hha	antitoxin-toxin module	26	15	13
yccA	modulator of FtsH protease	25	16	11
yjfN	Predicted protein	71	34	27
yqaE	predicted membrane protein	11	11	4.4
Repressed by CpxAR				
csgDEFG	curli production	-17	-21	-14
efeU1,2	pseudogene of ferrous iron permease	-12	-16	-17
ompF	outer membrane porin F	-6.7	-5.0	-3.4

[a] Shown is the fold change in gene expression for each time point after addition of *m*-Tyr divided by the time point just prior to *m*-Tyr addition (i.e. t=0). For activated genes, fold change is calculated as t=X min/t=0 min; for repressed genes, fold change is calculated as –(t=0 min/t=X min). Time points are minutes after the addition of *m*-Tyr. The fold-change is shown for just the first gene in the operon. All fold-changes meet the cut-off for significance of $p<0.005$.

Table 3. *m*-Tyr^R strains and their mutations in the three major sources of *m*-Tyr resistance.

Mutant Strain	Total # of Mutations[a]	Mutations[b]		
		aroP	*rhtC*	*tyrA*
Rmt1	17	W436C		
Rmt2	46	Q42(Am)		
Rmt3	3	S298F		
Rmt4	14		C(-43)T	
Rmt5	9		C(-43)T	
Rmt6	43	W100(Op)		
Rmt7	19		C(-43)T	
Rmt8	5			G106S

[a]Number of non-silent and intergenic SNPs identified by whole genome sequencing. SNPs were identified with a minimum requirement of 5x coverage of a given base and 80% agreement on the mutation.

[b]Mutations identified as being the major contributors to the strains' resistance to *m*-Tyr. Amino acid residue substitutions in the *aroP* and *tyrA* gene products is indicate by the single amino acid code for the original residue, followed by the codon number, and then the substituted resiude. If the codon is change to a stop codon, the nature of the stop codon is indicated as amber (Am) or opal (Op). For the *rhtC* gene, the mutation was outside the codon region, and the change is indicated as the original base, the location relative to the start of the gene, followed by the subsitutied base.

References

[1] Nunn PB, Bell EA, Watson AA, Nash RJ. Toxicity of non-protein amino acids to humans and domestic animals. Nat Prod Commun. 2010;5:485-504.
[2] Rodgers KJ. Non-protein amino acids and neurodegeneration: the enemy within. Exp Neurol. 2014;253:192-6.
[3] Bullwinkle T, Lazazzera B, Ibba M. Quality control and infiltration of translation by amino acids outside of the genetic code. Annu Rev Genet. 2014;48:149-66.
[4] Stadtman ER. Oxidation of free amino acids and amino acid residues in proteins by radiolysis and by metal-catalyzed reactions. Annu Rev Biochem. 1993;62:797-821.
[5] Huang T, Jander G, de Vos M. Non-protein amino acids in plant defense against insect herbivores: representative cases and opportunities for further functional analysis. Phytochemistry. 2011;72:1531-7.
[6] Wang X, Pan T. Stress Response and Adaptation Mediated by Amino Acid Misincorporation during Protein Synthesis. Adv Nutr. 2016;7:773S-9S.
[7] Jakubowski H. Quality control in tRNA charging. Wiley Interdiscip Rev RNA. 2012;3:295-310.
[8] Ling J, Reynolds N, Ibba M. Aminoacyl-tRNA synthesis and translational quality control. Annu Rev Microbiol. 2009;63:61-78.
[9] Moghal A, Mohler K, Ibba M. Mistranslation of the genetic code. FEBS Lett. 2014;588:4305-10.
[10] Martinis SA, Boniecki MT. The balance between pre- and post-transfer editing in tRNA synthetases. FEBS Lett. 2010;584:455-9.
[11] Jakubowski H. Quality control in tRNA charging -- editing of homocysteine. Acta Biochim Pol. 2011;58:149-63.
[12] Wong FC, Beuning PJ, Silvers C, Musier-Forsyth K. An isolated class II aminoacyl-tRNA synthetase insertion domain is functional in amino acid editing. J Biol Chem. 2003;278:52857-64.
[13] An S, Musier-Forsyth K. Trans-editing of Cys-tRNAPro by Haemophilus influenzae YbaK protein. J Biol Chem. 2004;279:42359-62.
[14] Ahel I, Korencic D, Ibba M, Soll D. Trans-editing of mischarged tRNAs. Proc Natl Acad Sci U S A. 2003;100:15422-7.
[15] Perona JJ, Gruic-Sovulj I. Synthetic and Editing Mechanisms of Aminoacyl-tRNA Synthetases. In: Kim S, editor. Aminoacyl-tRNA Synthetases in Biology and Medicine. Dordrecht: Springer Netherlands; 2014. p. 1-41.
[16] Moor N, Klipcan L, Safro MG. Bacterial and eukaryotic phenylalanyl-tRNA synthetases catalyze misaminoacylation of tRNA(Phe) with 3,4-dihydroxy-L-phenylalanine. Chem Biol. 2011;18:1221-9.
[17] Calendar R, Berg P. The catalytic properties of tyrosyl ribonucleic acid synthetases from Escherichia coli and Bacillus subtilis. Biochemistry. 1966;5:1690-5.
[18] Bullwinkle TJ, Reynolds NM, Raina M, Moghal A, Matsa E, Rajkovic A, et al. Oxidation of cellular amino acid pools leads to cytotoxic mistranslation of the genetic code. Elife. 2014;3.

[19] Klipcan L, Moor N, Kessler N, Safro MG. Eukaryotic cytosolic and mitochondrial phenylalanyl-tRNA synthetases catalyze the charging of tRNA with the meta-tyrosine. Proc Natl Acad Sci U S A. 2009;106:11045-8.
[20] Klipcan L, Finarov I, Moor N, Safro MG. Structural Aspects of Phenylalanylation and Quality Control in Three Major Forms of Phenylalanyl-tRNA Synthetase. J Amino Acids. 2010;2010:983503.
[21] Kartvelishvili E, Peretz M, Tworowski D, Moor N, Safro M. Chimeric human mitochondrial PheRS exhibits editing activity to discriminate nonprotein amino acids. Protein Sci. 2016;25:618-26.
[22] Lin SX, Baltzinger M, Remy P. Fast kinetic study of yeast phenylalanyl-tRNA synthetase: role of tRNAPhe in the discrimination between tyrosine and phenylalanine. Biochemistry. 1984;23:4109-16.
[23] Roy H, Ling J, Alfonzo J, Ibba M. Loss of editing activity during the evolution of mitochondrial phenylalanyl-tRNA synthetase. J Biol Chem. 2005;280:38186-92.
[24] Ling J, So BR, Yadavalli SS, Roy H, Shoji S, Fredrick K, et al. Resampling and editing of mischarged tRNA prior to translation elongation. Mol Cell. 2009;33:654-60.
[25] Ling J, Yadavalli SS, Ibba M. Phenylalanyl-tRNA synthetase editing defects result in efficient mistranslation of phenylalanine codons as tyrosine. RNA. 2007;13:1881-6.
[26] Gurer-Orhan H, Ercal N, Mare S, Pennathur S, Orhan H, Heinecke JW. Misincorporation of free m-tyrosine into cellular proteins: a potential cytotoxic mechanism for oxidized amino acids. The Biochemical journal. 2006;395:277-84.
[27] Ipson BR, Fisher AL. Roles of the tyrosine isomers meta-tyrosine and ortho-tyrosine in oxidative stress. Ageing Res Rev. 2016;27:93-107.
[28] Mohler K, Mann R, Bullwinkle TJ, Hopkins K, Hwang L, Reynolds NM, et al. Editing of misaminoacylated tRNA controls the sensitivity of amino acid stress responses in Saccharomyces cerevisiae. Nucleic Acids Res. 2017;45:3985-96.
[29] Keseler IM, Mackie A, Santos-Zavaleta A, Billington R, Bonavides-Martinez C, Caspi R, et al. The EcoCyc database: reflecting new knowledge about Escherichia coli K-12. Nucleic Acids Res. 2016.
[30] Wasmer C, Benkemoun L, Sabate R, Steinmetz MO, Coulary-Salin B, Wang L, et al. Solid-state NMR spectroscopy reveals that E. coli inclusion bodies of HET-s(218-289) are amyloids. Angewandte Chemie (International ed in English). 2009;48:4858-60.
[31] Rokney A, Shagan M, Kessel M, Smith Y, Rosenshine I, Oppenheim AB. E. coli transports aggregated proteins to the poles by a specific and energy-dependent process. J Mol Biol. 2009;392:589-601.
[32] Zakataeva NP, Aleshin VV, Tokmakova IL, Troshin PV, Livshits VA. The novel transmembrane Escherichia coli proteins involved in the amino acid efflux. FEBS Lett. 1999;452:228-32.
[33] Kruse D, Kramer R, Eggeling L, Rieping M, Pfefferle W, Tchieu JH, et al. Influence of threonine exporters on threonine production in Escherichia coli. Applied microbiology and biotechnology. 2002;59:205-10.
[34] Sampathkumar P, Morrison JF. Chorismate mutase-prephenate dehydrogenase from Escherichia coli. Purification and properties of the bifunctional enzyme. Biochim Biophys Acta. 1982;702:204-11.
[35] Bullwinkle TJ, Ibba M. Translation quality control is critical for bacterial responses to amino acid stress. Proc Natl Acad Sci U S A. 2016;113:2252-7.

[36] Charlier D, Roovers M, Van Vliet F, Boyen A, Cunin R, Nakamura Y, et al. Arginine regulon of Escherichia coli K-12. A study of repressor-operator interactions and of in vitro binding affinities versus in vivo repression. J Mol Biol. 1992;226:367-86.
[37] McLean S, Bowman LA, Sanguinetti G, Read RC, Poole RK. Peroxynitrite toxicity in Escherichia coli K12 elicits expression of oxidative stress responses and protein nitration and nitrosylation. J Biol Chem. 2010;285:20724-31.
[38] Jeeves M, Evans PD, Parslow RA, Jaseja M, Hyde EI. Studies of the Escherichia coli Trp repressor binding to its five operators and to variant operator sequences. Eur J Biochem. 1999;265:919-28.
[39] Pittard AJ, Davidson BE. TyrR protein of Escherichia coli and its role as repressor and activator. Molecular microbiology. 1991;5:1585-92.
[40] Zer H, Mizrahi H, Malchenko N, Avin-Wittenberg T, Klipcan L, Ostersetzer-Biran O. The Phytotoxicity of. Front Plant Sci. 2020;11:140.
[41] Meyer AS, Baker TA. Proteolysis in the Escherichia coli heat shock response: a player at many levels. Current opinion in microbiology. 2011;14:194-9.
[42] Raivio TL. Everything old is new again: an update on current research on the Cpx envelope stress response. Biochim Biophys Acta. 2014;1843:1529-41.
[43] Laskowska E, Wawrzynow A, Taylor A. IbpA and IbpB, the new heat-shock proteins, bind to endogenous Escherichia coli proteins aggregated intracellularly by heat shock. Biochimie. 1996;78:117-22.
[44] Allen SP, Polazzi JO, Gierse JK, Easton AM. Two novel heat shock genes encoding proteins produced in response to heterologous protein expression in Escherichia coli. Journal of bacteriology. 1992;174:6938-47.
[45] Ratajczak E, Zietkiewicz S, Liberek K. Distinct activities of Escherichia coli small heat shock proteins IbpA and IbpB promote efficient protein disaggregation. J Mol Biol. 2009;386:178-89.
[46] Tao J, Sang Y, Teng Q, Ni J, Yang Y, Tsui SK, et al. Heat shock proteins IbpA and IbpB are required for NlpI-participated cell division in Escherichia coli. Frontiers in microbiology. 2015;6:51.
[47] Govers SK, Dutre P, Aertsen A. In vivo disassembly and reassembly of protein aggregates in Escherichia coli. Journal of bacteriology. 2014;196:2325-32.
[48] Neeli-Venkata R, Martikainen A, Gupta A, Goncalves N, Fonseca J, Ribeiro AS. Robustness of the Process of Nucleoid Exclusion of Protein Aggregates in Escherichia coli. Journal of bacteriology. 2016;198:898-906.
[49] Winkler J, Seybert A, Konig L, Pruggnaller S, Haselmann U, Sourjik V, et al. Quantitative and spatio-temporal features of protein aggregation in Escherichia coli and consequences on protein quality control and cellular ageing. EMBO J. 2010;29:910-23.
[50] Rodgers KJ, Shiozawa N. Misincorporation of amino acid analogues into proteins by biosynthesis. Int J Biochem Cell Biol. 2008;40:1452-66.
[51] Ipson BR, Green RA, Wilson JT, Watson JN, Faull KF, Fisher AL. Tyrosine aminotransferase is involved in the oxidative stress response by metabolizing. J Biol Chem. 2019;294:9536-54.
[52] Bhosale SB, Rood JI, Sneddon MK, Morrison JF. Production of chorismate mutase-prephenate dehydrogenase by a strain of Escherichia coli carrying a multicopy, tyrA plasmid. Isolation and properties of the enzyme. Biochim Biophys Acta. 1982;717:6-11.

[53] Bertin C, Weston LA, Huang T, Jander G, Owens T, Meinwald J, et al. Grass roots chemistry: meta-tyrosine, an herbicidal nonprotein amino acid. Proc Natl Acad Sci U S A. 2007;104:16964-9.
[54] Huang T, Tohge T, Lytovchenko A, Fernie AR, Jander G. Pleiotropic physiological consequences of feedback-insensitive phenylalanine biosynthesis in Arabidopsis thaliana. Plant J. 2010;63:823-35.
[55] Miller JH. Experiments in molecular genetics: Cold Spring Harbor Laboratory; 1972.
[56] Li H, Durbin R. Fast and accurate short read alignment with Burrows-Wheeler transform. Bioinformatics. 2009;25:1754-60.
[57] Li H, Handsaker B, Wysoker A, Fennell T, Ruan J, Homer N, et al. The Sequence Alignment/Map format and SAMtools. Bioinformatics. 2009;25:2078-9.
[58] Chan W, Costantino N, Li R, Lee SC, Su Q, Melvin D, et al. A recombineering based approach for high-throughput conditional knockout targeting vector construction. Nucleic Acids Res. 2007;35:e64.
[59] Costantino N, Court DL. Enhanced levels of lambda Red-mediated recombinants in mismatch repair mutants. Proc Natl Acad Sci U S A. 2003;100:15748-53.
[60] Trapnell C, Pachter L, Salzberg SL. TopHat: discovering splice junctions with RNA-Seq. Bioinformatics. 2009;25:1105-11.
[61] Anders S, Pyl PT, Huber W. HTSeq--a Python framework to work with high-throughput sequencing data. Bioinformatics. 2015;31:166-9.
[62] Love MI, Huber W, Anders S. Moderated estimation of fold change and dispersion for RNA-seq data with DESeq2. Genome Biol. 2014;15:550.
[63] Schneider CA, Rasband WS, Eliceiri KW. NIH Image to ImageJ: 25 years of image analysis. Nat Methods. 2012;9:671-5.
[64] Schindelin J, Arganda-Carreras I, Frise E, Kaynig V, Longair M, Pietzsch T, et al. Fiji: an open-source platform for biological-image analysis. Nat Methods. 2012;9:676-82.

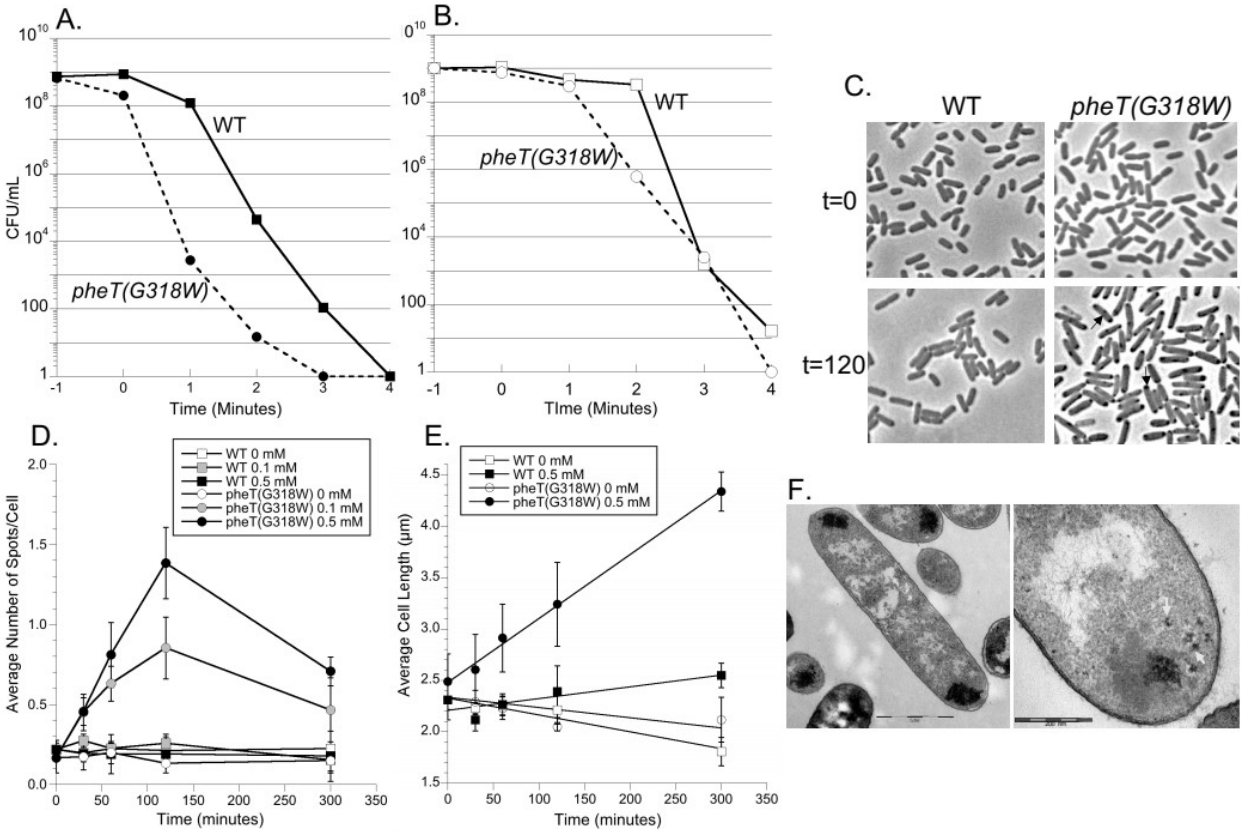

Figure 1. *m*-Tyr-treated *pheT(G318W)* editing-defective *E. coli* cells are heat sensitive and exhibit protein aggegation. Both wild-type *E. coli* (BAL4704; WT) and an *E. coli* strain expressing an editing-defective PheRS (BAL4073; *pheT(G318W)*) were grow in the presence and absence of *m*-Tyr. Circle symbols represent the *pheT(G318W)* stain, square symbols represent the WT strain, filled symbols indicate with *m*-Tyr, and open symbols indicate without *m*-Tyr. (A) shows that the PheRS editing defective strain dies more quickly than WT when exposed to a heat stress after being grown in the presence of *m*-Tyr. (B) There is no significant difference in the death rate when the strains are grown in the absence of *m*-Tyr. Time in minutes indicates the time prior (negative number) and after (positive numbers) of the culture reaching 60°C. Show is data from one representative of three independent experiments. The WT and *pheT(G318W)* strains were grown in M9 minimal media to an OD_{600} of 0.5 (t=0) and then dosed

with *m*-Tyr to a concentration of 0.5 mM. (C) DIC microscopy analysis of cells prior to (t=0) and 120 minutes (t=120) after the addition of *m*-Tyr. Black arrows indicate location of polar spots. Quantification of dark, polar spots per cell (D) and of cell length (E) versus the time after the addition of the indicated concentration of *m*-Tyr. Data points are averages of three biological replicates, with 50 cells per replicate, and the error bars are standard deviation of the mean. (F) Transmission electron microscopy of cells inclubed with *m*-Tyr for 120 minutes. Large protein aggregates localized to the poles. In some cases, small satellite dark spots around the main protein aggregate were observed (white arrows).

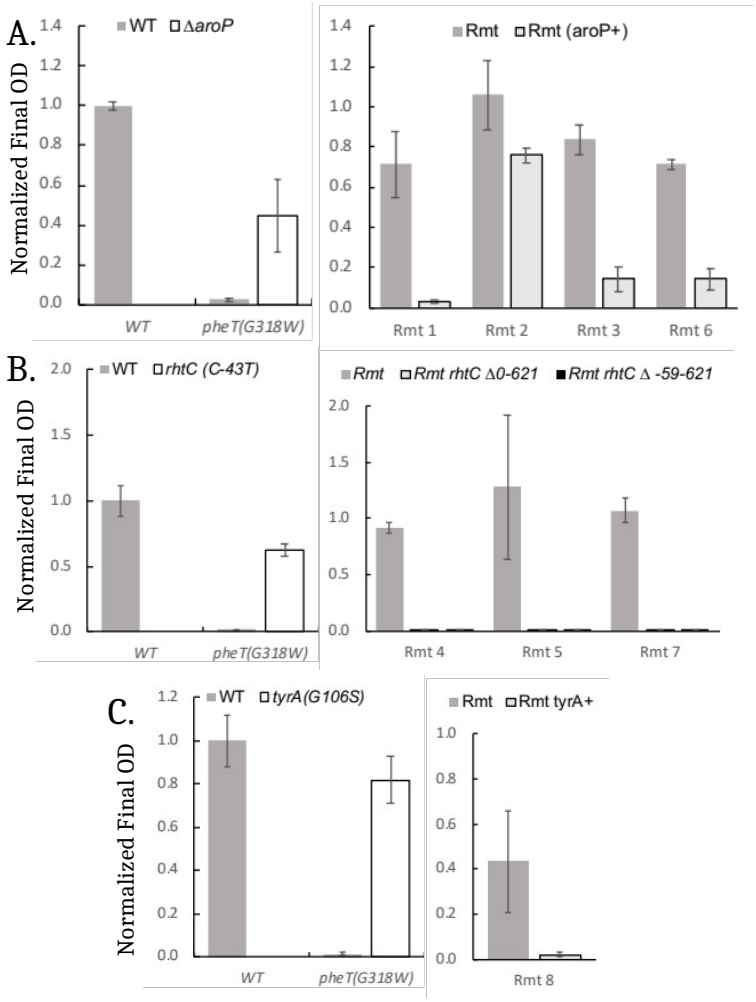

Figure 2. Mutations in *aroP*, *rhtC,* and *tyrA* cause resistance to *m*-Tyr. A.) Removal of *aroP* (ΔaroP) in a *pheT(G318W)* strain imparted *m*-Tyr^R. Strains Rmt1, Rmt3, and Rmt6 had the majority of their *m*-Tyr resistance eliminated when their mutant *aroP* alleles were replaced with the WT version (aroP+). **B.)** Introducing the *rhtC(C-43T)* mutation into a *pheT(G318W)* strain imparted resistance to *m*-Tyr. Deleting the coding region of the *rhtC* gene (*rhtC Δ0-621*) or elimination the promoter mutation and the *rhtC* gene (*rhtC* Δ *-59-621*) from Rmt mutant strains 4, 5 and 7 eliminated resistance to *m*-Tyr. **C.)** Reversion of the *tyrA(G106S)* mutation in the Rmt8 mutant strain to wild-type *tyrA* (*tyrA+*) eliminated resistance to *m*-Tyr. Conversely, when the *tyrA(G106S)* mutation was introduced into the *pheT(G318W)* strain, the resulting strain

exhibited *m*-Tyr^{R}. Bars are the average of three biological repeats. Error bars are standard deviation.